Journal of Alloys and Compounds xxx (2015) xxx–xxx

Contents lists available at ScienceDirect

Journal of Alloys and Compounds

journal homepage: www.elsevier.com/locate/jalcom

Shape-and size-controlled Ag nanoparticles stabilized by *in situ* generated secondary amines

E. Ramírez-Meneses [a,*], V. Montiel-Palma [b], M.A. Domínguez-Crespo [c], M.G. Izaguirre-López [c], E. Palacios-Gonzalez [d], H. Dorantes-Rosales [e]

[a] *Departamento de Ingeniería y Ciencias Químicas, Universidad Iberoamericana, Prolongación Paseo de la Reforma 880, Lomas de Santa Fe, Distrito Federal C.P. 01219, Mexico*
[b] *Centro de Investigaciones Químicas, Universidad Autónoma del Estado de Morelos, Av. Universidad 1001 Col. Chamilpa, Cuernavaca, Morelos C.P. 62209, Mexico*
[c] *Centro de Investigación en Ciencia Aplicada y Tecnología Avanzada-IPN, Unidad Altamira. Km 14.5 Carretera Tampico-Puerto Industrial, 89600 Altamira, Tamaulipas, Mexico*
[d] *Laboratorio de Microscopia de Ultra alta Resolución, Instituto Mexicano del Petróleo, Eje Central Lázaro Cárdenas No. 152, C.P. 07730 México D.F., Mexico*
[e] *Departamento de Metalurgia, E.S.I.Q.I.E.-I.P.N., Unidad Profesional Adolfo López Mateos, Zacatenco, Delegación. Gustavo A. Madero, C.P. 07738 México D.F., Mexico*

ARTICLE INFO

Article history:
Available online xxxx

Keywords:
Ag nanoparticles
Chemical synthesis
Amines
Stabilizers

ABSTRACT

Silver amides such as $AgN^{i}Pr_2$ and $AgN(SiMe_3)_2$ have been employed successfully as precursors for the yield synthesis of silver nanoparticles under mild conditions of dihydrogen gas reduction (2 atm) in organic media. Transmission electron microscopy (TEM) showed the formation of silver nanoparticles with FCC structure, variously sized from 26 to 35 nm for $AgN^{i}Pr_2$ and from 14 to 86 nm for $AgN(SiMe_3)_2$, the synthesis could take place in absence of added stabilizers due to the *in situ* formation of secondary amines from the reaction of dihydrogen gas with the amide ligands of the silver precursor. Indeed, the presence of HNR_2 (R = $i$$Pr_2$, $N(SiMe_3)_2$) on the surface of the nanoparticle was confirmed by spectroscopic means.

Finally, the addition of ethylenediamine as additional capping agent allowed not only the control of the structural characteristics of the resulting Ag nanoparticles (well-dispersed with spherical shape), but that regarding the nanoparticle size as it inhibited overgrowth, limiting it to *ca.* 25 nm.

1. Introduction

Metal nanoparticles (MNPs) with unusual chemical physical properties, often significantly different from those of their bulk counterparts, are undoubtedly the synthetic targets for nanoscience and engineering technology [1–8]. Furthermore, the focus of attention has not only been the synthesis of monodispersed nanoparticles, but also their self-organization into 2-dimensional (2-D) arrays [9–15]. Thus, one of the principal objectives of various synthetic strategies concerning metallic nanomaterials is to achieve a precise control of their size, shape and dispersion [16]. Among all metals, silver and gold are promising materials for their application in nonlinear optics as chemical sensors and optoelectronic nanodevices [17]. Ionic or metallic silver features low toxicity to human cells, high thermal stability and low volatility; such properties can be exploited in medicine for burning treatment and dental materials, and in the manufacturing industry as coatings for stainless steel materials, textile fabrics, water treatment, sunscreen lotions, etc. For the production of metallic silver from the cationic species, a variety of different reduction methods have been proposed such as γ-rays [18,19], ultraviolet or visible light [20], microwaves [21,22], ultrasonic radiation [23], electrochemical deposition [24], laser irradiation [25], thermal decomposition [26] and recently, hydrothermal methods [27]. As for the last methods, numerous reducing agents such as sodium borohydride ($NaBH_4$), formaldehyde, sodium citrate, hydrazine, ascorbic acid, glucose polysaccharides and even biological microorganisms [28–35] have been employed. To prevent the agglomeration and precipitation of silver nanoparticles, capping agents, either in organic or aqueous media, such as poly(vinylpyrrolidone) (PVP), poly(ethylene glycol) (PEG), oleic acid, dodecanoic acid, sodium citrate dehydrate, some surfactants and amines have been used [36–40].

In some cases, amines can serve as both reducing and capping agents. For instance, Mishra et al. [41] reported the synthesis of Ag nanomaterials with elongated structures in a two-phase system using hexadecylamine, whereas Chen et al. [42] obtained monodispersed silver nanoparticles (~12 nm) on a large scale in a simple oleylamine–liquid paraffin system. Oleylamine was also used as stabilizer by Hiramatsu and co-workers to obtain nearly monodispersed silver nanoparticles with variable size in the mixture of

* Corresponding author. Tel.: +52 (55) 9177 4400, +52 5950 4000x4057; fax: +52 (55) 5950 4279.
E-mail address: esther.ramirez@ibero.mx (E. Ramírez-Meneses).

http://dx.doi.org/10.1016/j.jallcom.2015.01.035
0925-8388/

oleylamine and toluene or hexane or dichlorobenzene [43]. Kashiwagi et al. [44] reported the synthesis of monodispersed silver NPs by heating a suspension of insoluble silver myristate in tertiary alkylamines at 80 °C. Alternatively, hexamethylenetetramine has been used as an efficient reducing agent [45]. More recently, triethylamine have been used as a promoted and directing agent for silver nanoparticles [46]. Others works have employed amines such as tetraethylenepentamine [8] and poly-amino compounds [47] as stabilizers.

Despite these advances regarding the accessibility of silver NPs, the use of alternative precursors to AgCl and $AgNO_3$ is much less developed with only a handful of reports using $AgClO_4$ [48], $Ag(CO_2C_6H_5CO_2)$ [18], $Ag(CH_3COO)$ [49], Ag(acac) [50], [Ag(μ-mesityl)]$_4$ [51] and more recently the organometallic $[Ag(C_6F_5)]$ [52]. However, it is evident that the selection of starting molecular precursors is crucial and often the most difficult task when targeting the controlled synthesis of nanoparticles. As for precursors, imposed requirements such as thermal stability, chemical selectivity and even solubility in non-polar organic media are often difficult to achieve from commercial or easily available precursors. Hence, apart from using organometallic compounds as nanoparticle sources, simple metal and metalloid amides, and in general element-nitrogen precursors, have very recently been proposed as alternative metal sources. Indeed, during the submission of this manuscript, a comprehensive review on the synthesis of colloidal nanocrystals and nanoparticles from metal and metalloid amides was published [53].

In this work, AgN^iPr_2 and $AgN(SiMe_3)_2$ have been proposed as practical alternative precursors to conventional $AgNO_3$ to form silver NPs under dihydrogen atmosphere either at room temperature or at 60 °C. The agglomeration of the nanoparticles was prevented by the *in situ* formation of the corresponding amines. The effect of the additional presence of capping agents such as ethylenediamine, $NH_2(CH_2)_2NH_2$ or hexamethyldisilazane and $HN(SiMe_3)_2$ on the size, shape and dispersion of the attained nanostructures was also studied. Although this is the first time silver amide precursors are used for this purpose, Chaudret et al. [54] employed previously analogous $Co[N(SiMe_3)_2]_2$ for the synthesis of Co nanoparticles.

2. Experimental

2.1. Synthesis of AgN^iPr_2 and $AgN(SiMe_3)_2$ precursors

The synthesis of AgN^iPr_2 was first reported by Lappert et al. [55] to proceed from the reaction of AgNCO and $M'[N(SiMe_3)_2]$ (were M′ = Sn, Pb, Yb). As for the present research work, AgN^iPr_2 and $AgN(SiMe_3)_2$ were prepared from either AgCl or $AgNO_3$ (Aldrich) using standard Schlenk and glove box techniques. Although $LiNR_2$ (R = $SiMe_3$) is commercially available, its fresh preparation (R = ^iPr) from the corresponding secondary amine (either diisopropilamine or hexamethyldisilazane) and stoichiometric amounts of a titrated n-BuLi (n-BuLi = C_4H_9Li) in hexanes was preferred. The white precipitate (either LiN^iPr_2 or $LiN(SiMe_3)_2$) was then filtered and dried under vacuum. Subsequently, a suspension of $LiNR_2$ (R = ^iPr, $N(SiMe_3)$) and one equivalent mol of AgCl in THF were vigorously stirred for 24 h at room temperature in darkness. The solution was filtered off the residue, concentrated to eliminate the remaining LiCl and recrystallized from THF. The general synthesis reaction of $AgNR_2$ precursors is presented in Fig. 1. The resulting compounds were insoluble in most common organic solvents, but gave satisfactory microanalytical data and FT-IR analysis.

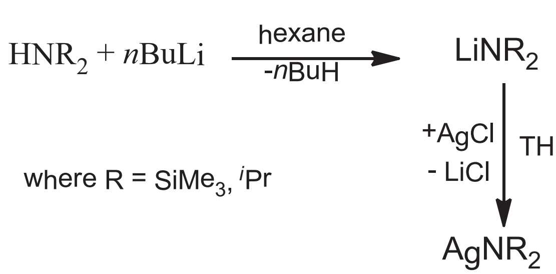

Fig. 1. General reaction of synthesis of $AgNR_2$ precursors.

2.2. Synthesis of Ag nanoparticles from AgN^iPr_2 and $AgN(SiMe_3)_2$

The synthesis of silver NPs was carried out in the darkness in a Fischer–Porter bottle either at room temperature or at 60 °C. A typical procedure is described below. AgN^iPr_2 or $AgN(SiMe_3)_2$ (40 mg) were introduced in a Fisher–Porter bottle under argon atmosphere and a mixture of freshly distilled and degassed tetrahydrofuran, THF (20 mL), and toluene (20 mL) was added. When an additional capping agent was needed, either 1 or 5 equivalents of it (either ethylenediamine or hexamethyldisilizane) were added at this point by means of a syringe. The obtained dark gray solutions were then pressurized under dihydrogen atmosphere (2 bar) for 16 h under stirring. After this time, homogeneous brown colloidal solutions were obtained. Schematic illustrations of the proposed stabilization of the silver NPs obtained from the AgN^iPr_2 and $AgN(SiMe_3)_2$ precursors are shown in Figs. 2 and 3, respectively.

2.3. Characterization of the as-synthesized silver nanoparticles

TEM specimens were prepared by slow evaporation of a drop of each crude colloidal solution deposited onto a holey carbon covered copper grid. Then, the colloidal solutions were purified by hexane washings (to eliminate the impurities). Finally, the resulting gray solution was evaporated in vacuum until the residue was completely dry. Size and morphology of the as-synthesized silver NPs were investigated by means of a JEOL-2000 FX II electron microscope, operating at 200 kV. The presence and bonding mode of the capping molecules after the purification step were studied through Fourier Transform-infrared spectroscopy (FT-IR, Spectrum One Perkin Elmer). KBr pellets (Aldrich, 99% IR grade) were employed to carry out this analysis.

3. Results and discussion

3.1. Ag nanoparticles from AgN^iPr_2 reduction

Fig. 4 illustrates typical transmission electron microscopy (TEM) images and their corresponding selected area electron diffraction (SAED) pattern of the silver nanoparticles obtained from the reaction of AgN^iPr_2 under H_2 atmosphere (2 bar) in the absence of additional capping agents either at room temperature or at 60 °C. From the TEM images, it can be observed spherical particles with no elongated or rod-shape. Regardless of the reaction temperature, the particle size distribution ranged from 20 to 50 nm. It is well documented that high reaction temperatures provoke important effects on the shape and size of nanoparticles, generally increasing the latter [42,56]. In our system, small Ag nanoparticles (<20 nm) were produced, displaying a very slight tendency to agglomerate at higher temperatures, i.e. the TEM micrograph in Fig. 4a shows the dispersion obtained when the synthesis was carried out at room temperature, which is slightly better than that obtained at 60 °C, where some aggregates of particles are formed (Fig. 4c). This behavior is in agreement with the stabilization of the silver NPs likely resulting from the coordination of solvent (THF) as well as of the *in situ* generated HN^iPr_2, both of which are volatile and will therefore be less efficient in preventing aggregation at higher temperatures. The corresponding SAED of the particles was identified and confirmed the silver FCC (face centered cubic) structure (JCPDS 04-0783), Fig. 4b. The average distances between the fringes and the corresponding crystallographic planes are presented in Table 1.

The Ag particles obtained at 60 °C show a different crystallographic plane (420) that is not observed in the case of the particles obtained at room temperature, Fig. 4d. These different lattice planes of the Ag crystals in the Ag nanoparticles could be attributed to alternative growth mechanisms dependent on temperature and the presence of the *in situ* generated HN^iPr_2. Thus, according to previous works, reaction temperature variations affect the particle growth mechanisms [57]. In our case, the synthesis carried out at 60 °C showed that the initial solution exhibited a color change from white to gray during the first 30 min and at room temperature, change

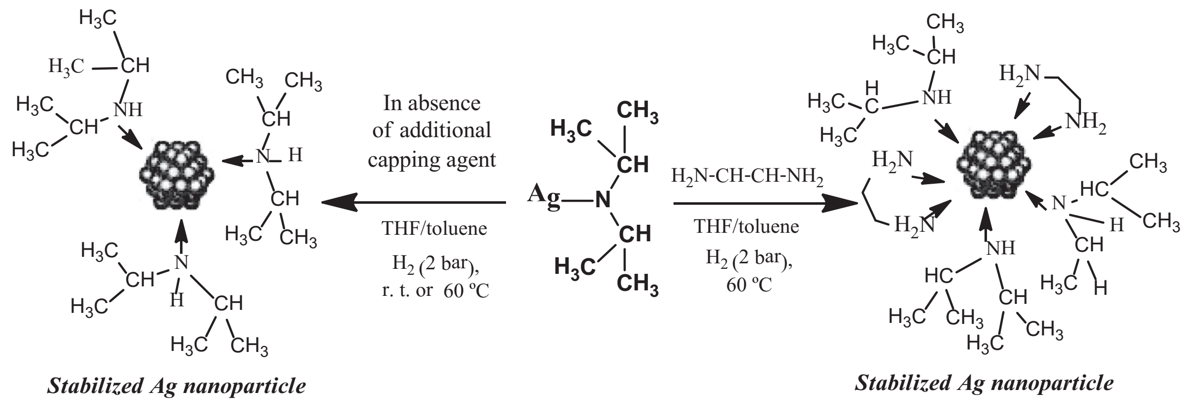

Fig. 2. Schematic illustration of the proposed stabilization of Ag nanoparticles obtained from $AgN^{i}Pr_2$ precursor in absence of additional capping agent (a) or in the presence of ethylenediamine as capping agent (b).

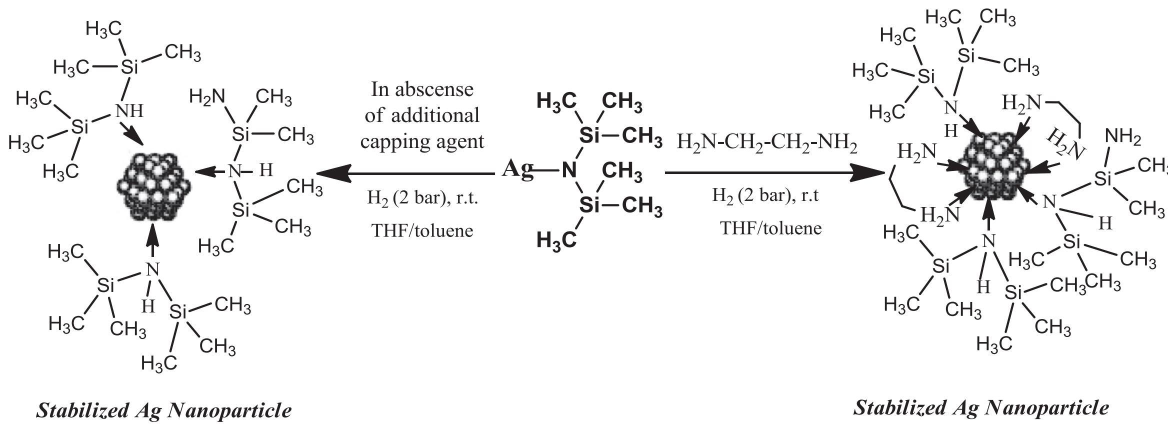

Fig. 3. Schematic illustration of the proposed formation of Ag nanoparticles obtained from $AgN(SiMe_3)_2$ precursor in absence of additional capping agent or in the presence of ethylenediamine or hexamethyldisilizane.

color was observed after 1 h. These observations seems to indicate that the rate of nucleation process and subsequent stage of nanoparticle growth are influenced by temperature [58,59].

FT-IR spectroscopy was used to validate both the formation of the amine ligand from the amide precursor and its presence after the purification step. It is expected that the amino group of the molecule acts as an electron donor group to the Ag particle surface, thus surrounding the particle, exposing the $HN^{i}Pr_2$ groups to the outside and constituting a steric hindrance for the metal particle growth. Fig. 5 shows FT-IR spectra corresponding to Ag nanoparticles synthesized at room temperature and 60 °C. The FT-IR spectrum of $AgN^{i}Pr_2$ is also shown as a reference. In the spectra of the synthesized nanoparticles, a band at ca. 3400 cm^{-1} is observed and it is attributed to the stretching mode of the amino functional group (–NH). A slight shift in the position of this band is observed when comparing the samples obtained at the two different reaction temperatures. The N–H bending scissoring absorption band was observed at around 1600 cm^{-1} in all the spectra of the NPs. Additionally, the band corresponding to the methyl asymmetric $\nu_{as}(CH_3)$ mode is observed at ca. 2961 cm^{-1} in the spectrum of free $AgN^{i}Pr_2$, while it is shifted to 2950 cm^{-1} and 2963 cm^{-1} for silver NPs synthesized at room temperature and at 60 °C, respectively. All of these findings are in agreement with the *in situ* formation of $HN^{i}Pr_2$ in the reaction media and account for the previously described stabilization.

Relatively small shifts in the IR bands of stabilizers upon coordination of the NPs surfaces have also been reported in systems such as oleylamine capped Ag NPs [42], PVP capped Ag NPs [60], dodecanethiol capped Ag nanocrystals [10] and nonanethiol passivated Ag NPs [61]. Some of these works state that the displacement is the consequence of the constraint of the capping molecular motions most likely resultant from the formation of a relatively close-packed amine layer on the surface of the Ag NPs [42,61].

The use of organic capping agents (also known as stabilizing or protecting agents) in the bottom-up approach is usually required during the synthesis of Ag nanopowders to control the material particle size, agglomeration, and morphology [62–64]. Previous works employed ethylenediamine as an efficient stabilizer of metal nanoparticles or even in quantum dots to preserve their surface properties acting as an assisted ligand exchange [65–69]. Thus, to evaluate the effect of additional capping agents during the synthesis of Ag nanoparticles, a series of experiments using $AgN^{i}Pr_2$ at 60 °C in presence of 1 or 5 equivalents of ethylenediamine ($NH_2(CH_2)_2NH_2$) was also performed. The morphology, particle size distribution and structure of the as-prepared Ag nanoparticles in presence of capping agents were analyzed by TEM with the corresponding SAED, and the results are shown in Fig. 6a–d. The micrographs show that the addition of capping agents exerts some effects on the size, dispersion and shape of the obtained Ag NPs in comparison with the samples synthesized in absence of additional capping agents. A noticeable change in shape from semi-spherical to spherical nanoparticles with some additional nanorods was observed. It is well known that a capping agent plays a twofold role: it acts as a stabilizing agent, preventing aggregation of metal particles and as a uniform colloidal dispersion keeper [70]. The average particle size using different amounts of ethylenediamine

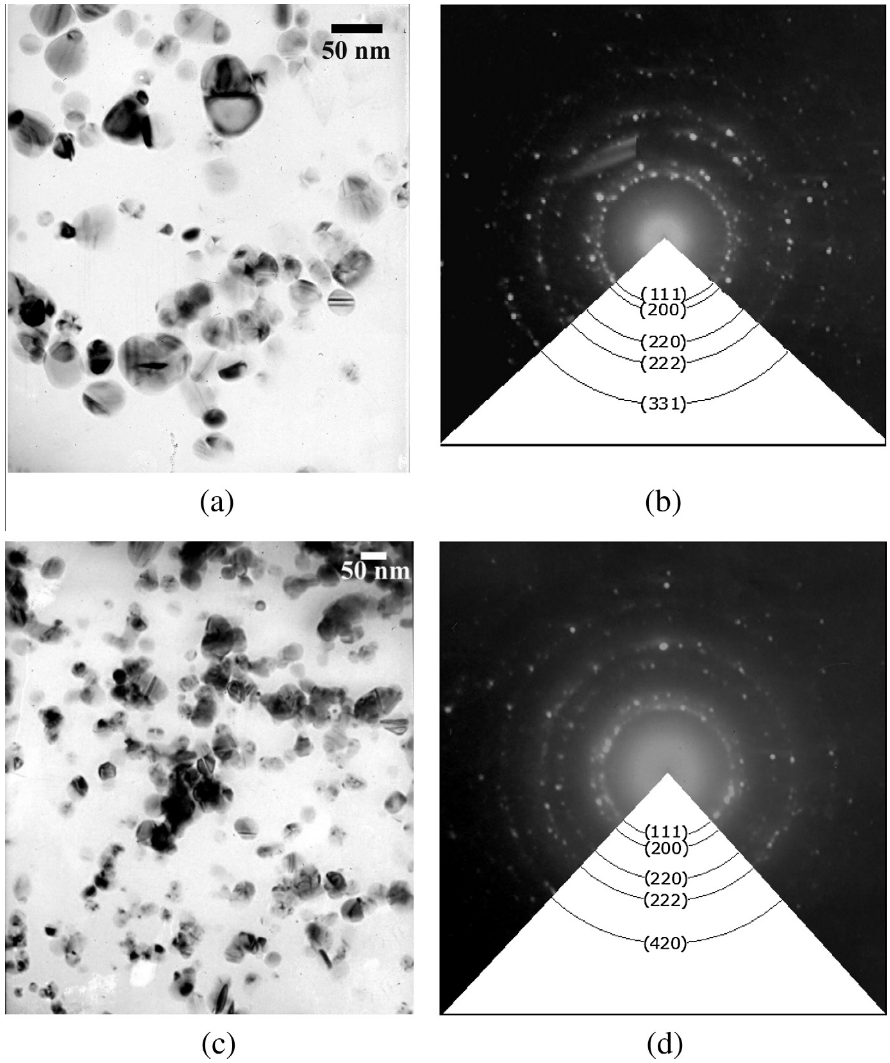

Fig. 4. TEM images and corresponding electron diffraction patterns of Ag nanoparticles obtained under dihydrogen (2 bars) from $AgN^{i}Pr_2$ in organic media in the absence of additional capping agents synthesized at room temperature (a,b) and 60 °C (c,d).

Table 1
Interplanar distances and planes of Ag nanoparticles obtained from $AgN^{i}Pr_2$.

Ag Nps obtained at r.t. SAED from Fig. 1b			Ag Nps obtained at 60 °C SAED from Fig. 1d		
in absence of additional capping agent					
d (Å)	*d* (Å) JCPDS file 04-0783	Planes	*d* (Å)	*d* (Å) JCPDS file 04-0783	Planes
2.33	2.3833	(111)	2.34	2.3833	(111)
2.04	2.0640	(200)	2.02	2.0640	(200)
1.42	1.4594	(220)	1.41	1.4594	(220)
1.19	1.1916	(222)	1.21	1.1916	(222)
0.902	0.9470	(331)	0.91	0.9230	(420)
Ag Nps at 60 °C in the presence of additional capping agent					
Ag Nps/1 equiv. of $NH_2(CH_2)_2NH_2$			Ag Nps /5 equiv. of $NH_2(CH_2)_2NH_2$		
d (Å)	*d* (Å) JCPDS file 04-0783	Planes	*d* (Å)	*d* (Å) JCPDS file 04-0783	Planes
2.33	2.3833	(111)	2.36	2.3833	(111)
2.02	2.0640	(200)	2.03	2.0640	(200)
1.42	1.4594	(220)	1.42	1.4594	(220)
1.17	1.1916	(222)	1.22	1.2446	(311)
0.91	0.9230	(420)	0.92	0.9230	(420)

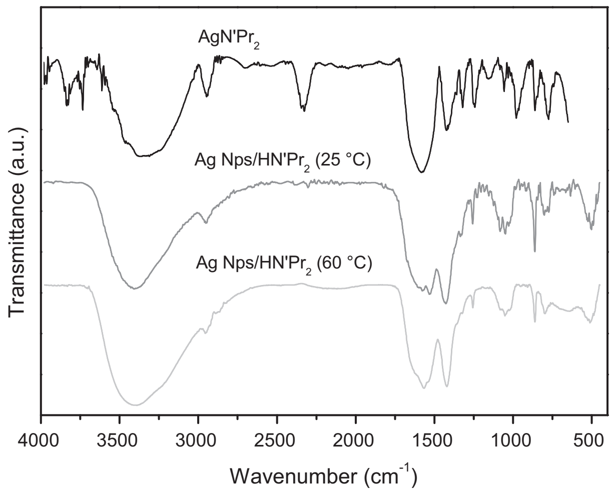

Fig. 5. FT-IR spectrum of AgN^iPr_2 precursor and spectra of Ag nanoparticles obtained from AgN^iPr_2 in organic media in the absence of additional capping agents synthesized at room temperature (25 °C) and 60 °C.

ranged from 10 to 30 nm, which are smaller than those obtained in the absence of additional capping agent (20–50 nm). It is important to notice that the amount of capping agent exerts an effect on the shape of the nanostructures; i.e. whereas mainly spherical shapes were observed when using 5 equivalents of ethylenediamine (Fig. 6c), nanorods and spherical nanostructures could be obtained with 1 equivalent (Fig. 6a). The corresponding SAED patterns (Fig. 6b–d) for the as-synthesized particles are consistent with the reported FCC silver structure (Table 1).

The corresponding FT-IR spectra of the Ag NPs synthesized in the presence of 1 and 5 equivalents of added ethylendiamine exhibit absorbing peaks at ~2900 cm^{-1}, corresponding to νN–H, Fig. 7. Once again, it seems that the broad band attributed to the amino group shifts to lower wavenumbers (~3200 cm^{-1}) as a result of the electron donation from the amino group to the silver surface.

3.2. Ag nanoparticles from $AgN(SiMe_3)_2$ as precursor

In order to evaluate the effect of the precursor on the shape and size of the Ag nanoparticles, a similar set of experiments was per-

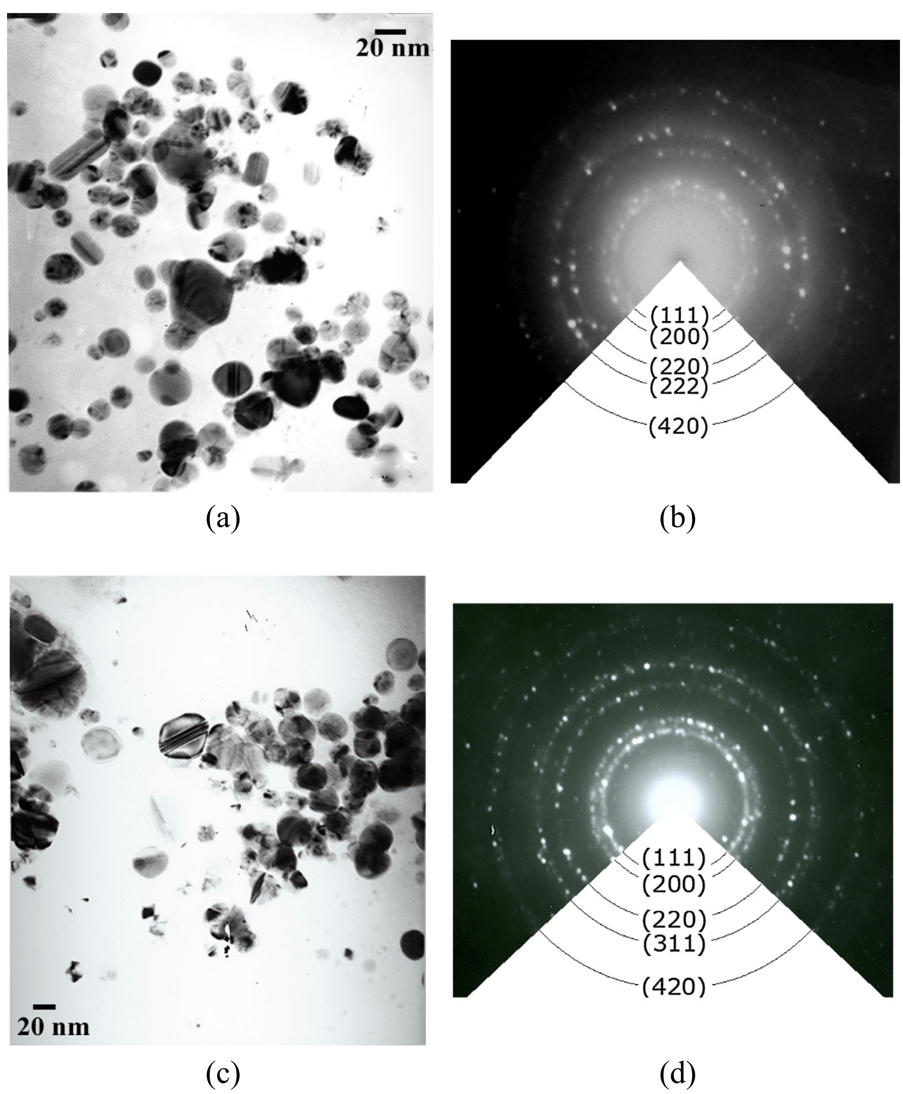

Fig. 6. TEM images of Ag nanoparticles obtained under dihydrogen (2 bars) from AgN^iPr_2 in organic media at 60 °C in the presence of (a) 1 equiv. and (c) 5 equiv. of ethylenediamine as capping agent and their corresponding typical electron diffraction patterns (b and d).

Please cite this article in press as: E. Ramírez-Meneses et al., J. Alloys Comp. (2015), http://dx.doi.org/10.1016/j.jallcom.2015.01.035

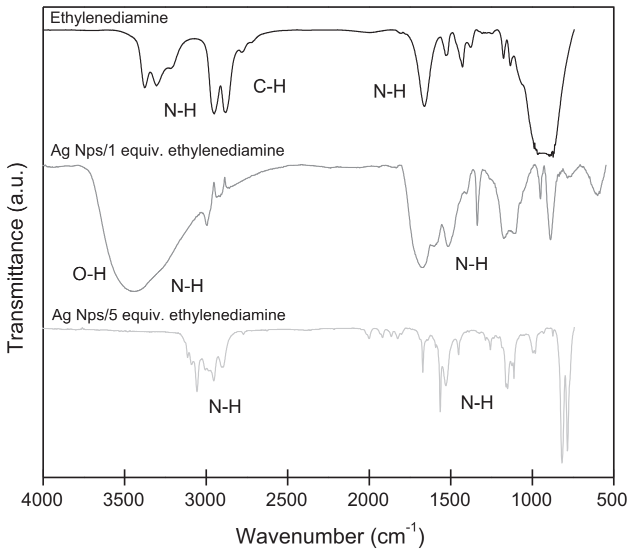

Fig. 7. FT-IR spectra for of Ag nanoparticles obtained under dihydrogen (2 bars) from $AgN^{i}Pr$ in organic media at 60 °C in the presence of ethylenediamine (1 and 5 equiv.) as additional capping agent.

formed using $AgN(SiMe_3)_2$ as a precursor. Fig. 8a–d shows TEM images of Ag nanoparticles obtained from $AgN(SiMe_3)_2$ without any additional capping agent at room temperature, under H_2 atmosphere (3 bar) and with different reaction times (16 and 240 h). After 16 h, polydispersed and agglomerated semispherical particles are observed (14 ± 8 nm, Fig. 8a and b). Under these conditions, the formed $HN(SiMe_3)_2$ molecules surround the particle, enabling a steric stabilization [71,72]. When the reaction mixture is left to react for longer times (240 h), the TEM images show a significant increase in the average particle size (86 ± 23 nm, Fig. 8c and d), characteristic of Ostwald ripening phenomena during the crystal growth process. Thus, polydispersed and spherical (or semi-spherical) Ag particles were obtained, Fig. 8c. From the similar shape and surface appearance observed in the micrographs of the Ag NPs obtained from either $AgN^{i}Pr_2$ or $AgN(SiMe_3)_2$, it can be inferred that the amine group functionality is responsible of the stabilization; on the other hand, the presence of either $HN^{i}Pr_2$ or $HN(SiMe_3)_2$ on the surface of the synthesized Ag NPs does not seem to exert a significant effect on their shape. Tao et al. [70] reported that fluxional structures have been considered to behave as reactors or templates during the synthesis. However, in this work, the relatively low concentration of ligands in the colloidal solution seems to limit the possibility of template formation.

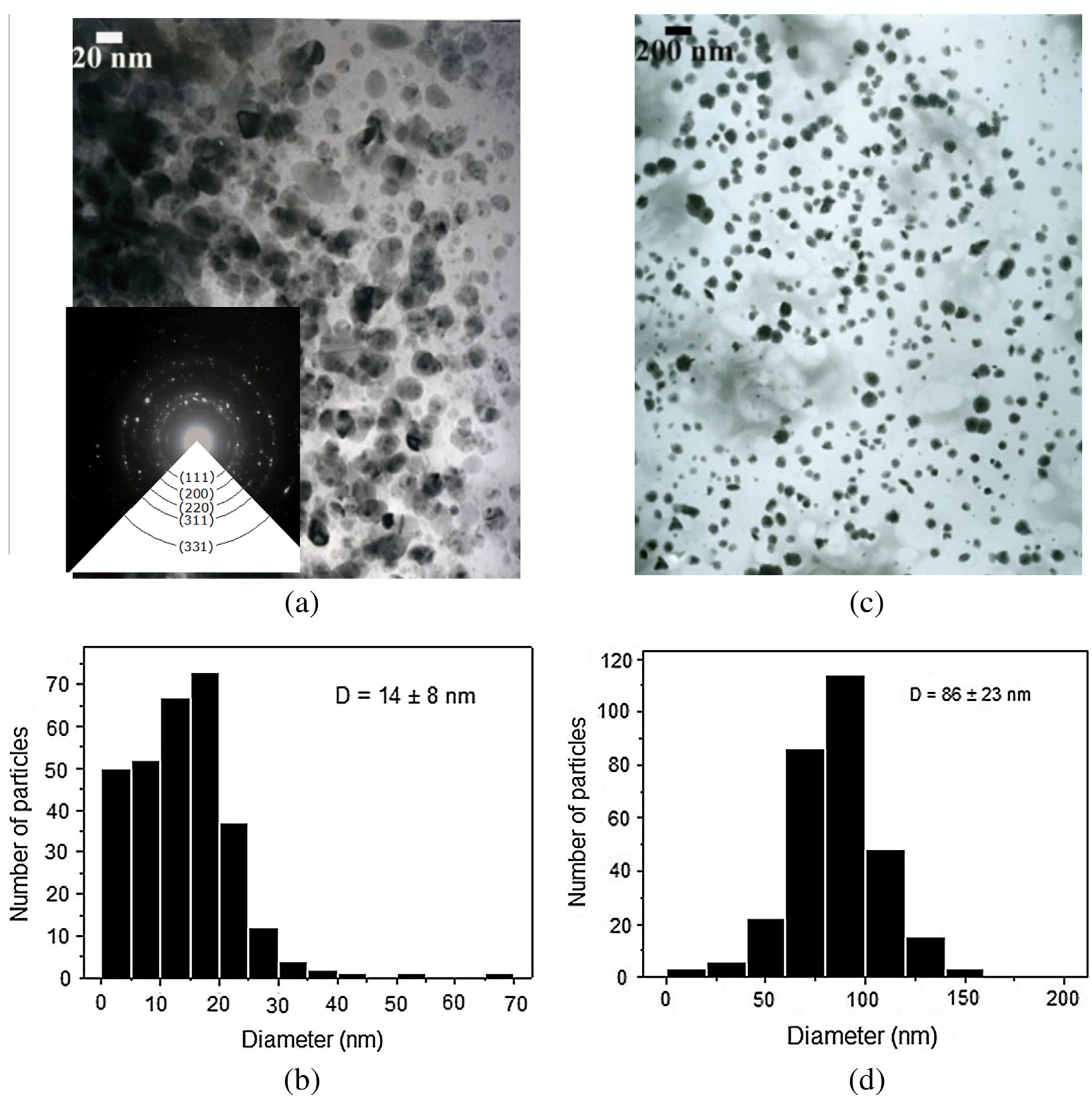

Fig. 8. TEM images and size distributions of Ag nanoparticles obtained from $AgN(SiMe_3)_2$ without additional capping agent at room temperature and its corresponding histograms of size distribution (inset typical electron diffraction pattern of Ag nanoparticles) with reaction time of 16 h (a and b) and 10 days (c and d).

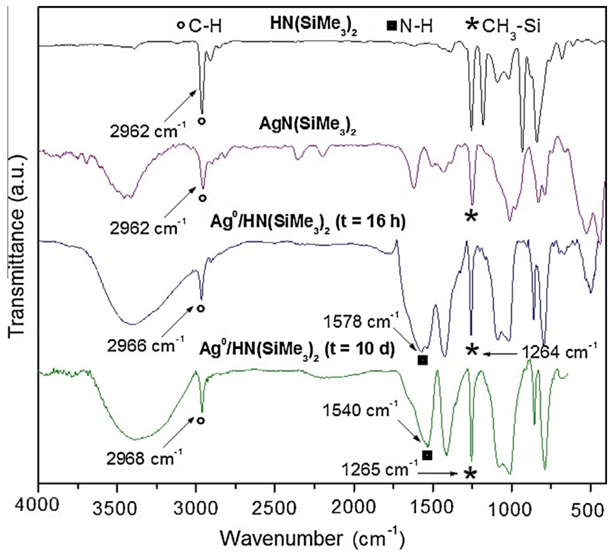

Fig. 9. FT-IR spectra of Ag nanoparticles obtained from $AgN(SiMe_3)_2$ without additional capping agent at r.t. with reaction times of 16 h and 10 days. Additionally, $AgN(SiMe_3)_2$ precursor and $HN(SiMe_3)_2$ as references.

Fig. 9 shows the FT-IR spectra of the Ag NPs obtained from $AgN(SiMe_3)_2$ without additional capping agent. Comparisons with the $AgN(SiMe_3)_2$ precursor and $HN(SiMe_3)_2$ were also analyzed, Fig. 9. The spectra corresponding to the Ag NPs/$HN(SiMe_3)_2$ systems for 16 and 240 h were qualitatively similar. The FT-IR spectra of $HN(SiMe_3)_2$ and $AgN(SiMe_3)_2$, displayed, in both cases, $\nu_{as}(CH_3)$ at c.a. 2962 cm^{-1}. In the Ag NPs/$HN(SiMe_3)_2$ systems, however, this peak is slightly shifted by 4 and 6 cm^{-1}: $\nu_{as}(CH_3)$ = 2966 cm^{-1} and $\nu_{as}(CH_3)$ = 2968 cm^{-1}. This relatively small shift has also been reported in the case of oleylamine-capped silver colloids, dodecanethiol-capped Ag nanocrystals and nonanethiol-passivated Ag nanoparticles and can be correlated to the constraint of the capping molecular motions [42]. Additionally, the peak at ~1580 cm^{-1}, corresponding to N–H in the $AgN(SiMe_3)_2$ spectra, also appeared shifted in the Ag NPs/$HN(SiMe_3)_2$ systems at 1578 and 1540 cm^{-1}, in agreement with the coordination of the ligand on the silver surface [54]. The band positions of Si–CH_3 bending and stretching modes of Ag NPs/$HN(SiMe_3)_2$ systems also appeared shifted towards higher wavenumbers (1–2 cm^{-1}) in comparison with the corresponding $AgN(SiMe_3)_2$ precursor and $HN(SiMe_3)_2$ (~800 and ~1260 cm^{-1}), which is once more in agreement with capping molecular motions of these ligands on the surface of the Ag NPs.

The synthesis of Ag NPs from $AgN(SiMe_3)_2$ was also carried out by adding a certain amount of $HN(SiMe_3)_2$ as a supplementary capping agent. The addition of it was expected to provoke a better dispersion or even a particle size reduction. Fig. 10 shows TEM images of the as-synthesized Ag nanoparticles obtained after 16 and 240 h of reaction time in the presence of 1 equivalent of $HN(SiMe_3)_2$ (see Table 2). In both cases, agglomerates of Ag structures with a wide size distribution were obtained, most of them having undefined shapes. Ag structures obtained after 16 h presented an average particle size of 46 ± 17 nm, larger than those obtained in absence of added $HN(SiMe_3)_2$. Once again, longer reaction times (240 h) produced increased average sizes of silver structures of 58 ± 27 nm. Thus, the presence of added $HN(SiMe_3)_2$ added to the reaction media is not as effective as it is the addition of HN^iPr_2, probably due to larger steric hindrance in the latter and/or to different growth mechanisms. Although it is proposed that the particle surface is covered by either amine, in line with the proposal made for analogous Co systems [54], the presence of additional $HN(SiMe_3)_2$ from the beginning of the reaction seems to disrupt the organization of reaction media, letting the formation of Ag structures that are bigger than those obtained in the absence of additional amine. These series of experiments demonstrate the predominant role of chemical equilibrium between coordinating agents such as the ligands resulting from the precursor and additional amines for stabilizing Ag structures.

Significant differences are observed when the syntheses are performed in the presence of additional 5 equivalents of a supplementary stabilizer such as ethylenediamine. Indeed, the TEM analyses demonstrate that the obtained nanoparticles have a defined shape (spherical) and are well dispersed. The effect of the supplementary stabilizing agent can also be noted in the diminished particle size of the Ag nanostructures (25 ± 10 nm) with respect to the systems of added $HN(SiMe_3)_2$, Fig. 11. Although the size could be considered to be slightly larger than those obtained in the absence of any added stabilizer (14 ± 8 nm, Fig. 8a and b), it should be noted that in this case, dispersion is improved and no agglomeration is present, Fig. 11. Thus, the addition of ethylenediamine allows the enhanced control of the properties of the particles. Moreover, the morphology results (spherical) are comparable with the nature of the particles when AgN^iPr_2 was used as a precursor in the presence of 1 equivalent of ethylendiamine (Fig. 6). The ethylendiamine role preventing nanoparticle agglomeration has also been observed in Ru systems in aqueous environment [73].

The presence of nanoparticle-coordinated ethylendiamine is supported by the IR spectra of the obtained nanoparticles which present similar but shifted bands with respect to those obtained with pure ethylenediamine, Fig. 12. Indeed, slightly higher wavenumbers in the bands corresponding to N–H vibrations suggest the amine coordination to the Ag nanoparticles on the surface

Table 2
Interplanar distances and planes of Ag nanoparticles obtained from $AgN(SiMe_3)_2$ in the presence of hexamethyldisilazane as additional capping agent.

Ag Nps obtained at r.t. and *t* = 16 h SAED from Fig. 10b			Ag Nps obtained at r.t and *t* = 10 days SAED from Fig. 10d		
d (Å)	*d* (Å) JCPDS file 04-0783	Planes	*d* (Å)	*d* (Å) JCPDS file 04-0783	Planes
2.43	2.3833	(111)	2.40	2.3833	(111)
2.04	2.0640	(200)	2.00	2.0640	(200)
1.43	1.4594	(220)	1.44	1.4594	(220)
1.23	1.2446	(311)	1.22	1.2446	(311)
		–			–
		–			–
0.93	0.9400	(331)			–
		–	0.91	0.9230	(420)
		–			–

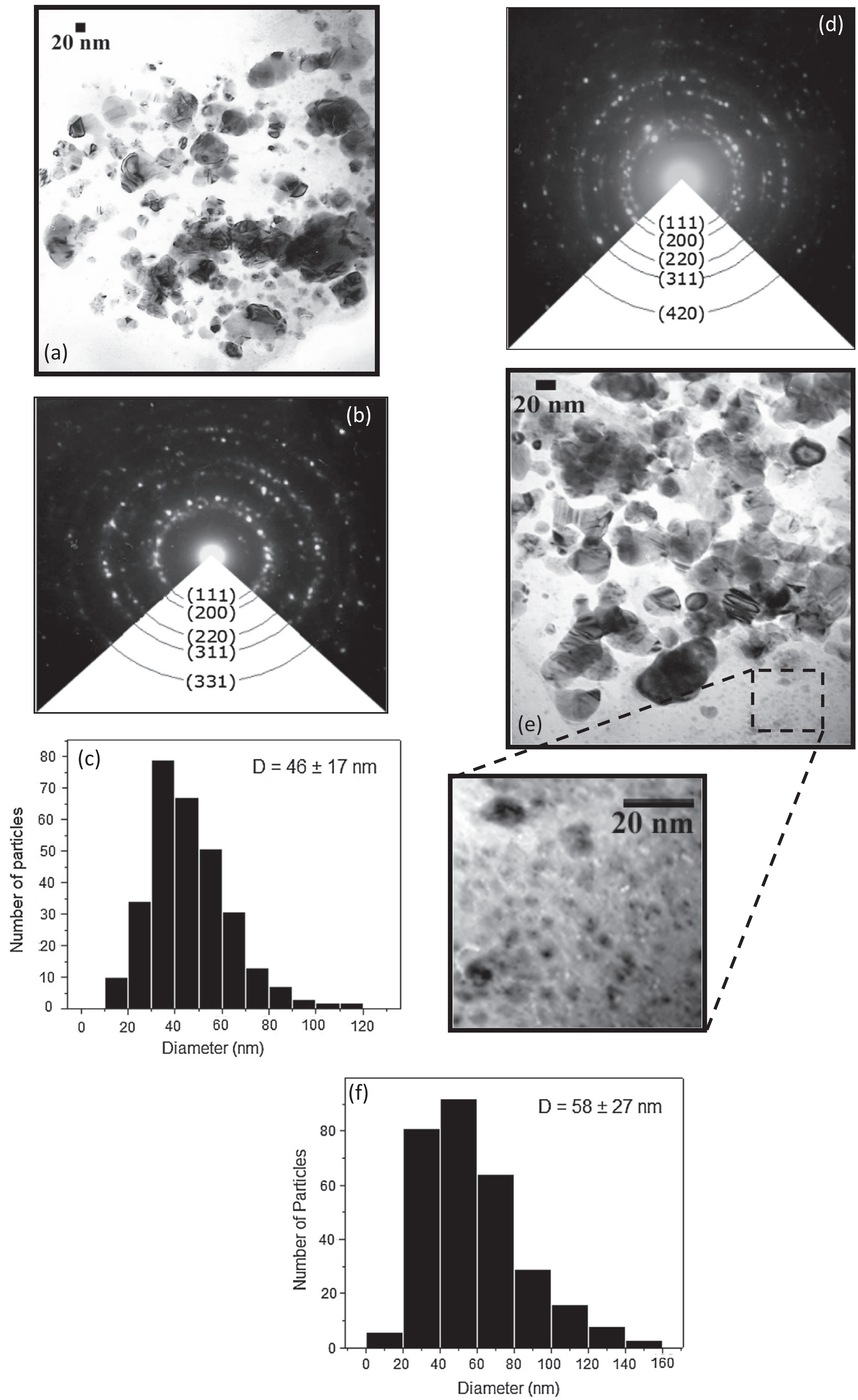

Fig. 10. TEM images, corresponding electron diffraction patterns and histograms of size distribution of Ag nanoparticles obtained under dihydrogen (2 bars) from $AgN(SiMe_3)_2$ precursor in the presence of 1 equivalent of hexamethyldisilazane as additional capping agent synthesized at 16 h (a–c) and 10 days (d–f).

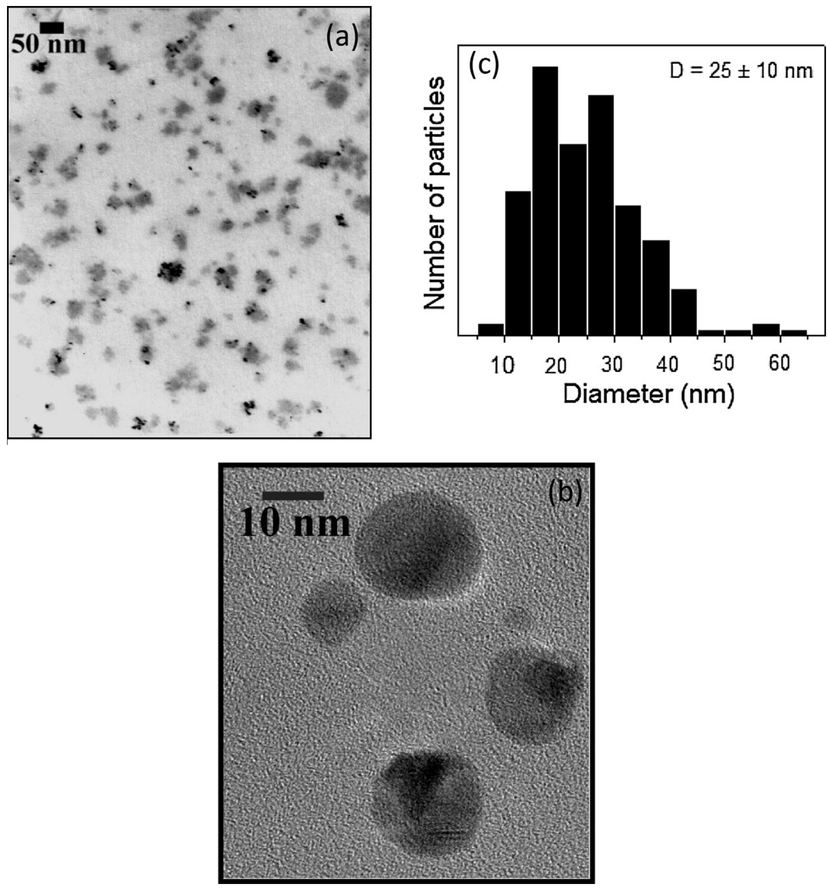

Fig. 11. TEM images of Ag nanoparticles obtained from $AgN(SiMe_3)_2$ at room temperature in the presence of 5 equiv. of ethylenediamine as capping agent (a and b) and its corresponding histogram of size distribution of Ag nanoparticles.

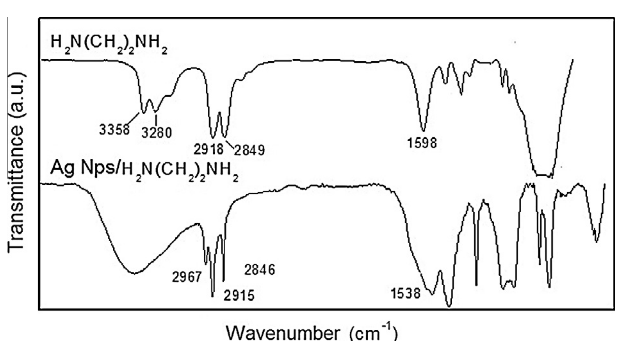

Fig. 12. FT-IR spectra of ethylenediamine and stabilized Ag nanoparticles obtained from $AgN(SiMe_3)_2$ at room temperature in the presence of 5 equivalents of ethylenediamine.

[72]. It both spectra, the correspondence between the bands due to the N–H bond vibration at ca. at 3360 and 3280 cm^{-1} as well as the band at 1598 cm^{-1} is evident. The same is true for the stretching C–H vibrations of CH_2 groups at ca. 2920 and 2850 cm^{-1}.

4. Conclusions

Silver nanoparticles were synthesized successfully from silver amide complexes such as AgN^iPr_2 and $AgN(SiMe_3)_2$ by reduction with dihydrogen (2 bar) using two different temperatures: room temperature and 60 °C. FT-IR spectra showed that the as-prepared silver nanoparticles are stabilized by *in situ* generated HN^iPr_2 or $HN(SiMe_3)_2$. The Ag nanoparticles synthesized from AgN^iPr_2 displayed sizes ranging from 26 to 35 nm, however, the synthesis temperature did not affect significantly the size distribution or shape of the Ag nanostructures.

The addition of 1 or 5 equivalents of ethylenediamine as additional capping agent notably decreased the average size of the particles with respect to that obtained from the Ag NPs/HN^iPr_2 system. On the other hand, Ag nanostructures obtained from the $AgN(SiMe_3)_2$ precursor, polydispersed and agglomerated semi-spherical particles from ~14 to 86 nm, are observed in the absence of additional capping agent. Nevertheless, when 1 equivalent of $HN(SiMe_3)_2$ is added as supplementary capping agent, agglomerates of Ag structures with undefined shape and wide size distribution were obtained. The presence of additional $HN(SiMe_3)_2$ must disrupt the organization of the reaction media, enabling the formation of Ag structures that are bigger in size than those obtained in the absence of additional amine.

The interaction of the amine molecules with the silver nanoparticle surface is quite strong, but the exact nature of the interaction is not fully understood at this time. However its incorporation to the reaction media helped obtain well dispersed spherical particles with ca. 25 nm in size. Based on these observations, ethylenediamine must favor the formation of spherical particles due to the coordination between amine groups and the silver surface.

Acknowledgments

The authors wish to acknowledge the financial support provided by CONACyT through the 105762 and 157613 projects, Universidad Iberoamericana 0053 project and SNI-CONACyT. The research was conducted in the framework of the "French-Mexican International Laboratory (LIA) LCMMC

References

[1] M.C. Daniel, D. Astruc, Gold nanoparticles: assembly, supramolecular chemistry, quantum-size-related properties, and applications toward biology, catalysis, and nanotechnology, Chem. Rev. 104 (2004) 293–346.

[2] L.N. Lewis, Chemical catalysis by colloids and clusters, Chem. Rev. 93 (1993) 2693–2730.

[3] A.C. Templeton, D.E. Cliffel, R.W. Murray, Redox and fluorophore functionalization of water-soluble, tiopronin-protected gold clusters, J. Am. Chem. Soc. 121 (1999) 7081–7089.

[4] R. Elghanian, Selective colorimetric detection of polynucleotides based on the distance-dependent optical properties of gold nanoparticles, Science 277 (1997) 1078–1081.

[5] S.A. Maier, M.L. Brongersma, P.G. Kik, S. Meltzer, A.A.G. Requicha, H.A. Atwater, Plasmonics – a route to nanoscale optical devices, Adv. Mater. 13 (2001) 1501–1505.

[6] L.M. Liz-Marzan, D.J. Norris, M.G. Bawendi, T. Betley, H. Doyle, P. Guyot-Sionnest, V.I. Klimov, N.A. Kotov, P. Mulvaney, C.B. Murray, D.J. Schiffrin, M. Shim, S. Sun, C. Wang, New aspects of nanocrystal research, MRS Bull. 26 (2001) 981–984.

[7] Y. Li, F. Qian, J. Xiang, C.M. Lieber, Nanowire electronic and optoelectronic devices, Mater. Today 9 (2006) 18–27.

[8] J. Xiong, X.-D. Wu, Q.-J. Xue, One-step route for the synthesis of monodisperse aliphatic amine-stabilized silver nanoparticles, Colloids Surf. A: Physicochem. Eng. Aspects 423 (2013) 89–97.

[9] R.L. Whetten, J.T. Khoury, M.M. Alvarez, S. Murthy, I. Vezmar, Z. Wang, P.W. Stephens, Ch.L. Clevend, W.D. Luedtke, U. Landman, Nanocrystal gold molecules, Adv. Mater. 8 (1996) 428–433.

[10] B.A. Korgel, S. Fullam, S. Connolly, D. Fitzmaurice, Assembly and self-organization of silver nanocrystal superlattices: ordered "soft spheres", J. Phys. Chem. B 102 (1998) 8379–8388.

[11] J.H. Fendler, Nanoparticles and Nanostructured Films, Wiley-VCH, Germany, Weinhem, 1998.

[12] G. Duan, W. Cai, Y. Luo, Y. Li, Y. Lei, Hierarchical surface rough ordered Au particle arrays and their surface enhanced Raman scattering, Appl. Phys. Lett. 89 (2006) 181918.

[13] M.M. Miranada, B. Pergolese, A. Bigotto, A. Giusti, Stable and efficient silver substrates for SERS spectroscopy, J. Colloid Interface Sci. 314 (2007) 540–544.

[14] A.M. Schwartzberg, C.D. Grant, A. Wolcott, C.E. Talley, T.R. Huser, R. Bogomolni, J.Z. Zhang, Unique gold nanoparticle aggregates as a highly active surface-enhanced Raman scattering substrate, J. Phys. Chem. B 108 (2004) 19191–19197.

[15] Z. Zhang, M. Han, One-step preparation of size-selected and well-dispersed silver nanocrystals in polyacrylonitrile by simultaneous reduction and polymerization, J. Mater. Chem. 13 (2003) 641–643.

[16] T.S. Ahmadi, Z.L. Wang, T.C. Green, A. Henglein, M.A. El-Sayed, Shape controlled synthesis of colloidal platinum nanoparticles, Science 272 (1996) 1924–1925.

[17] U. Kreibig, M. Gartz, A. Hilger, H. Hovel, Optical investigations of surfaces and interfaces of metal clusters, Adv. Met. Semicond. Clust. 4 (1998) 345–393.

[18] A. Henglein, M. Giersig, Formation of colloidal silver nanoparticles: capping action of citrate, J. Phys. Chem. B 103 (1999) 9533–9539.

[19] T. Li, H.G. Park, S.-H. Choi, Γ-Irradiation-induced preparation of Ag and Au nanoparticles and their characterizations, Mater. Chem. Phys. 105 (2007) 325–330.

[20] M. Darroudi, M.B. Ahmad, A. Khorsand Zak, R. Zamiri, M. Hakimi, Fabrication and characterization of gelatin stabilized silver nanoparticles under UV-light, Int. J. Mol. Sci. 12 (2011) 6346–6356.

[21] X. Jiang, W.M. Chen, C.Y. Chen, S.X. Xiong, A.B. Yu, Role of temperature in the growth of silver nanoparticles through a synergetic reduction approach, Nanoscale Res. Lett. 6 (2011) 32–40.

[22] A. Khan, A.M. El-Toni, S. Alrokayan, M. Alsalhi, M. Alhoshan, A.S. Aldwayyan, Microwave-assisted synthesis of silver nanoparticles using poly-nisopropylacrylamide/acrylic acid microgel particles, Colloids Surf. A: Physicochem. Eng. Aspects 377 (2011) 356–360.

[23] G.W. Yang, H. Li, Sonochemical synthesis of highly monodispersed and size controllable Ag nanoparticles in ethanol solution, Mater. Lett. 62 (2008) 2189–2191.

[24] D. Manno, E. Filippo, M. Di Giulio, A. Serra, Synthesis and characterization of starch-stabilized Ag nanostructures for sensors applications, J. Non-Crystalline Solids 354 (2008) 5515–5520.

[25] J.P. Abid, A.W. Wark, P.F. Brevet, H.H. Girault, Preparation of silver nanoparticles in solution from a silver salt by laser irradiation, Chem. Commun. (2002) 792–793

[26] S. Navaladian, B. Viswanathan, R.P. Viswanath, T.K. Varadarajan, Thermal decomposition as route for silver nanoparticles, Nanoscale Res. Lett. 2 (2007) 44–48.

[27] Z. Liu, Z. Xing, Y. Zu, S. Tan, L. Zhao, Z. Zhou, T. Sun, Synthesis and characterization of L-histidine capped silver nanoparticles, Mater. Sci. Eng. C 32 (2012) 811–816.

[28] K.S. Chou, Y.C. Lu, H.H. Lee, Effect of alkaline ion on the mechanism and kinetics of chemical reduction of silver, Mater. Chem. Phys. 94 (2005) 429–433.

[29] D.G. Shchukin, I.L. Radtchenko, G.B. Sukhorukov, Photoinduced reduction of silver inside microscale polyelectrolyte capsules, Chem. Phys. Chem. 4 (2003) 1101–1103.

[30] J. Xu, X.-W. Wei, X.-J. Song, X.-J. Lu, C.-C. Ji, Y.-H. Ni, G.-C. Zhao, Synthesis and electrocatalytic activity of multi-walled carbon nanotubes/Cu–Ag nanocomposites, J. Mater. Sci. 42 (2007) 6972–6976.

[31] Y.G. Sun, B. Mayers, T. Herricks, Y.N. Xia, Polyol synthesis of uniform silver nanowires: a plausible growth mechanism and the supporting evidence, Nano Lett. 3 (2003) 955–960.

[32] G. Li, D. He, Y. Qian, B. Guan, S. Gao, Y. Cui, K. Yokoyama, L. Wang, Fungus-mediated green synthesis of silver nanoparticles using *Aspergillus terreus*, Int. J. Mol. Sci. 13 (2012) 466–476.

[33] D. Philip, Green synthesis of gold and silver nanoparticles using *Hibiscus rosasinensis*, Physica E: Low-dimensional Syst. Nanostruct. 42 (2010) 1417–1424.

[34] P.U. Rani, P. Rajasekharreddy, Green synthesis of silver–protein (core–shell) nanoparticles using *Piper betle* L. leaf extract and its ecotoxicological studies on *Daphnia magna*, Colloids Surf. A: Physicochem. Eng. Aspects 389 (2011) 188–194.

[35] Abou El-Nour, M.M. Kholoud, Ala'a Eftaiha, Abdulrhman Al-Warthan, Reda A.A. Ammar, Synthesis and applications of silver nanoparticles, Arabian J. Chem. 3 (2010) 135–140.

[36] P.K. Khanna, V.S. Subbarao, Nanosized silver powder via reduction of silver nitrate by sodium formaldehydesulfoxylate in acidic pH medium, Mater. Lett. 57 (2003) 2242–2245.

[37] X. Qing, C. Xing, Z. Kai, L. Jinhuai, Synthesis and characterizations of polycrystalline walnut-like CdS nanoparticle by solvothermal method with PVP as stabilizer, Mater. Chem. Phys. 111 (2008) 98–105.

[38] K.J. Lee, B.H. Jun, J. Choi, Y.-I. Lee, J. Joung, Y.S. Oh, Environmentally friendly synthesis of organic-soluble silver nanoparticles for printed electronics, Nanotechnology 18 (2007) 335601–335604.

[39] K.J. Lee, Y.-I. Lee, I.-K. Shim, J. Joung, Y.S. Oh, Direct synthesis and bonding origins of monolayer-protected silver nanocrystals from silver nitrate through in situ ligand exchange, J. Colloids Interface Sci. 304 (2006) 92–97.

[40] G. Von White II, P. Kerscher, R.M. Brown, J.D. Morella, W. McAllister, D. Dean, C.L. Kitchens, Green synthesis of robust biocompatible silver nanoparticles using garlic extract, J. Nanomaterials (2012). ID730746.

[41] T. Mishra, R.K. Sahu, S.-H. Lim, L.G. Salamanca-Riba, S. Bhattacharjee, Hexadecylamine capped silver and gold nanoparticles: comparative study on formation and self-organization, Mater. Chem. Phys. 123 (2010) 540–545.

[42] M. Chen, Y.-G. Feng, X. Wang, T.C. Li, J.-Y. Zhang, D.-J. Qian, Silver nanoparticles capped by oleylamine: formation, growth, and self-organization, Langmuir 23 (2007) 5296–5304.

[43] H. Hiramatsu, F.E. Osterloh, A simple large-scale synthesis of nearly monodisperse gold and silver nanoparticles with adjustable sizes and with exchangeable surfactants, Chem. Mater. 16 (2004) 2509–2511.

[44] Y. Kashiwagi, M. Yamamoto, M. Nakamoto, Facile size-regulated synthesis of silver nanoparticles by controlled thermolysis of silver alkylcarboxylates in the presence of alkylamines with different chain lengths, J. Colloids Interface Sci. 300 (2006) 169–175.

[45] G.-P. Yong, D. Tian, H.-W. Tong, S.-M. Liu, Mesoporous SBA-15 supported silver nanoparticles as environmentally friendly catalysts for three-component reaction of aldehydes, alkynes and amines with glycol as a "green" solvent, J. Mol. Catal. A: Chem. 323 (2010) 40–44.

[46] E. Filippo, A. Serra, A. Buccolieri, D. Manno, Controlled synthesis and chain-like self-assembly of silver nanoparticles through tertiary amine, Colloids Surf. A: Physicochem. Eng. Aspects 417 (2013) 10–17.

[47] J. Xiong, X.-D. Wu, Q.-J. Xue, One-step synthesis of highly monodisperse silver nanoparticles using poly-amino compounds, Colloids Surf. A: Physicochem. Eng. Aspects 441 (2014) 109–115.

[48] H.-W. Wang, H.-C. Lin, C.-H. Kuo, Y.-L. Cheng, Y.-C. Yeh, Synthesis and photocatalysis of mesoporous anatase TiO_2 powders incorporated Ag nanoparticles, J. Phys. Chem. Solids 69 (2008) 633–636.

[49] P. Jeevanandam, C.K. Srikanth, S. Dixit, Synthesis of monodisperse silver nanoparticles and their self-assembly through simple thermal decomposition approach, Mater. Chem. Phys. 122 (2010) 402–407.

[50] S. Scirè, C. Crisafulli, S. Giuffrida, C. Mazza, P.M. Riccobene, A. Pistone, Supported silver catalysts prepared by deposition in aqueous solution of Ag nanoparticles obtained through a photochemical approach, Appl. Catal. A: Gen. 367 (2009) 138–145.

[51] S.D. Bunge, T.J. Boyle, T.J. Headley, Synthesis of coinage-metal nanoparticles from mesityl precursors, Nano Lett. 3 (2003) 901–905.

[52] J. Crespo, J. García-Barrasa, J.M. López-de-Luzuriaga, M. Monge, M.E. Olmos, Y. Sáenz, C. Torres, Organometallic approach to polymer-protected antibacterial silver nanoparticles: optimal nanoparticle size-selection for bacteria interaction, J. Nanoparticle Res. 14 (2012) 1281–1284.

[53] M. Yarema, R. Caputo, M.V. Kovalenko, Precision synthesis of colloidal inorganic nanocrystals using metal and metalloid amines, Nanoscale 5 (2013) 8398–8410.

[54] (a) B. Chaudret, Organometallic approach o nanoparticles synthesis and selforganization, C.R. Physique 6 (2005) 117–131.
(b) O. Margeat, C. Amiens, B. Chaudret, P. Lecante, R.E. Benfield, Chemical control of structural and magnetic properties of cobalt nanoparticles, Chem. Mater. 17 (2005) 107–111.

[55] P.B. Hitchcok, M.F. Lappert, L.J.M. Pierssens, Synthesis and X ray molecular structures of the silver(I) amides [{Ag[μ-N(SiMe$_3$)$_2$]}$_4$] and [{Ag[μ-NCMe$_2$(CH$_2$)$_3$CMe$_2$]}$_4$], Chem. Commun. (1996) 1189–1190
[56] C. Luo, Y. Zhang, X. Zeng, Y. Zeng, Y. Wang, The role of poly(ethylene glycol) in the formation of silver nanoparticles, J. Colloid Interface Sci. 288 (2005) 444–448.
[57] H. Jiang, K. Moon, Z. Zhang, S. Pothukuchi, C.P. Wong, Variable frequency microwave synthesis of silver nanoparticles, J. Nanoparticle Res. 8 (2006) 117–124.
[58] A. Panáček, R. Prucek, J. Hrbáč, T. Nevečná, J. Šteffková, R. Zbořil, L. Kvitek, Polyacrylate-assisted size control of silver nanoparticles and their catalytic activity, Chem. Mater. 26 (2014) 1332–1339.
[59] S.K. Volkman, S. Yin, T. Bakhishev, K. Puntambekar, V. Subramanian, M.F. Toney, Mechanistic studies on sintering of silver nanoparticles, Chem. Mater. 23 (2011) 4634–4640.
[60] H. Wang, X. Qiao, J. Chen, X. Wang, S. Ding, Mechanisms of PVP in the preparation of silver nanoparticles, Mater. Chem. Phys. 94 (2005) 449–453.
[61] S.T. He, J.N. Yao, S.S. Xie, H.J. Gao, S.J. Pang, Superlattices of silver nanoparticles passivated by mercaptan, J. Phys. D: Appl. Phys. 34 (2001) 3425–3429.
[62] T.M. Tolaymat, A.M. El Badawy, A. Genaidy, K.G. Scheckel, T.P. Luxton, M. Suidan, An evidence-based environmental perspective of manufactured silver nanoparticle in syntheses and applications: a systematic review and critical appraisal of peer-reviewed scientific papers, Sci. Total Environ. 408 (2010) 999–1006.
[63] M. Chen, Y.G. Feng, X. Wang, T.C. Li, J.Y. Zhang, D.J. Qian, Silver nanoparticles capped by oleylamine: formation, growth, and self-organization, Langmuir 23 (2007) 5296–5304.
[64] X. Fu, W. Yu, Y. Lin, D. Wang, H. Shi, F. Yan, Preparation of concentrated stable fluids containing silver nanoparticles in nonpolar organic solvent, J. Disper. Sci. Technol. 26 (2005) 575–580.
[65] M.-Q. Dai, L.-Y. Lanry Yung, Ethylenediamine-assisted ligand exchange and phase transfer of oleophilic quantum dots: stripping of original ligands and preservation of photoluminescence, Chem. Mater. 25 (2013) 2193–2201.
[66] B. Feng, J. Yang, J. Cao, L. Yang, M. Gao, M. Wei, Y. Liu, H. Song, Controllable synthesis, growth mechanism and optical properties of the ZnSe quantum dots and nanoparticles with different crystalline phases, Mater. Res. Bull. 48 (2013) 1040–1044.
[67] N.A. Ray, R.P. Van Duyne, P.C. Stair, Synthesis strategy for protected metal nanoparticles, J. Phys. Chem. C 116 (2012) 7748–7756.
[68] D. Lin, H. Liu, K. Qian, X. Zhou, L. Yang, J. Liu, Ultrasensitive optical detection of trinitrotoluene by ethylenediamine-capped gold nanoparticles, Anal. Chim. Acta 744 (2012) 92–98.
[69] J.Y. Lee, J. Yang, T.C. Deivaraj, H.-P. Too, A novel synthesis route for ethylenediamine-protected ruthenium nanoparticles, J. Colloids Interface Sci. 268 (2003) 77–80.
[70] A.R. Tao, S. Habas, P. Yang, Shape control of colloidal metal nanocrystals, Small 4 (2008) 310–325.
[71] A. Roucoux, J. Schulz, H. Patin, Reduced transition metal colloids: a novel family of reusable catalysts?, Chem Rev. 102 (2002) 3757–3778.
[72] M.V. Roldán, N.S. Pellegri, O.A. de Sanctis, Optical response of silver nanoparticles stabilized by amines to LSPR based sensors, Proc. Mater. Sci. 1 (2012) 594–600.
[73] J. Yang Lee, J. Yang, T.C. Deivaraj, H.-P. Too, A novel synthesis route for ethylenediamine-protected ruthenium nanoparticles, J. Colloid Interface Sci. 268 (2003) 77–80.

Please cite this article in press as: E. Ramírez-Meneses et al., J. Alloys Comp. (2015), http://dx.doi.org/10.1016/j.jallcom.2015.01.035